Sensors and Actuators B 215 (2015) 568–576

Contents lists available at ScienceDirect

Sensors and Actuators B: Chemical

journal homepage: www.elsevier.com/locate/snb

A highly selective turn-on chemosensor capable of monitoring Zn^{2+} concentrations in living cells and aqueous solution

Gyeong Jin Park[a], Hyun Kim[a], Jae Jun Lee[a], Yong Sung Kim[a], Sun Young Lee[a], Suyeon Lee[b], Insup Noh[b], Cheal Kim[a,*]

[a] Department of Fine Chemistry and Department of Interdisciplinary Bio IT Materials, Seoul National University of Science and Technology, Seoul 139-743, Republic of Korea
[b] Department of Chemical and Biomolecular Engineering, and Convergence Program of Biomedical Engineering and Biomaterials, Seoul National University of Science & Technology, Seoul 139-743, Republic of Korea

ARTICLE INFO

Article history:
Received 14 January 2015
Received in revised form 11 March 2015
Accepted 14 March 2015
Available online 17 April 2015

Keywords:
Fluorescence
Determination of Zn ion
Chemosensor
CHEF
Cell imaging

ABSTRACT

A new simple "off–on fluorescence type" chemosensor **1** (2-(*N*-(2-hydroxyethyl)-*N*-((pyridin-2-yl) methyl)amino)-*N*-(quinolin-8-yl)acetamide) has been synthesized for Zn^{2+}. The sensor **1** comprises of the quinoline as fluorophore and the 2-((pyridin-2-yl)methylamino)ethanol as both binding site and water-soluble functional group. **1** showed a remarkable fluorescence enhancement in the presence of Zn^{2+} in aqueous solution, which was reversible with the addition of ethylenediaminetetraacetic acid (EDTA). The detection limit (0.02 μM) of **1** for Zn^{2+} is far lower than World Health Organization guideline (76 μM) in drinking water. Importantly, the chemosensor **1** could be used to detect and quantify Zn^{2+} in living cells and water samples. Moreover, the sensing mechanism was supported by theoretical calculations. Therefore, this sensor has the ability to be a practical system for monitoring Zn^{2+} concentrations in biological and aqueous samples.

1. Introduction

The importance of transition metal ions in biological, environmental and chemical processes has affected the development of metal sensing field [1]. Among various metal ions, detecting zinc has been extensively studied [2], because the zinc ion is one of the most abundant transition-metal ions present in living cells, owing to its rich coordination chemistry [3]. In addition to its well-described vital role in catalytic centers and structural cofactors of many Zn^{2+}-containing enzymes and DNA-binding proteins, it plays important roles in various biological processes such as apoptosis, regulators of gene expression, and neural signal transmitters or modulators [4]. On the other hand, the deficiency of zinc causes unbalanced metabolism, which in turn can induce retarded growth in children, brain disorders and high blood cholesterol, and also be implicated in various neurodegenerative disorders such as Alzheimer's disease, epilepsy, ischemic stroke, and infantile diarrhea [5]. Consequently, selective detection and quantification for zinc ion are the very important object of increasing investigation [2a,6].

Although previous works have involved the development of a wide variety of chemical and physical sensors for the detection of Zn^{2+}, improving the detection selectivity among coexisting transition metal ions has been challenging. In addition, many of these methods require expensive equipment and involve time-consuming and laborious procedures that can be carried out only by trained professionals, significantly restricting the practical application of these Zn^{2+} sensors [7]. For convenience and low cost, easily-prepared Zn^{2+} fluorescence chemosensors are needed [8].

In view of this requirement and as part of our research effort devoted to zinc ion recognition, we have considered the combination of a quinoline moiety known as having desirable photo-physical properties as a fluorophore group and a 2-((pyridin-2-yl)methylamino)ethanol (**2**, see Scheme 1) unit with a pyridyl group and an ethanol group as a binding site [2a,9]. In particular, we expected that the ethanol group having a hydrophilic character would make water-solubility of a chemosensor increase. Finally, we synthesized a new type of water-soluble chemosensor **1** (Scheme 1) by combining the quinolone group with **2**, and tested its sensing properties towards various metal ions.

Herein, we present the synthesis of a new chemosensor composed of the quinoline fluorophore and 2-((pyridin-2-yl) methylamino)ethanol binding site. Sensor **1** showed an intense fluorescence enhancement in the presence of zinc ions in aqueous

* Corresponding author. Tel.: +82 2 970 6693; fax: +82 2 973 9149.
E-mail addresses: chealkim@seoultech.ac.kr, chealkim20@daum.net, chealkim@snut.ac.kr (C. Kim).

http://dx.doi.org/10.1016/j.snb.2015.03.108
0925-4005/

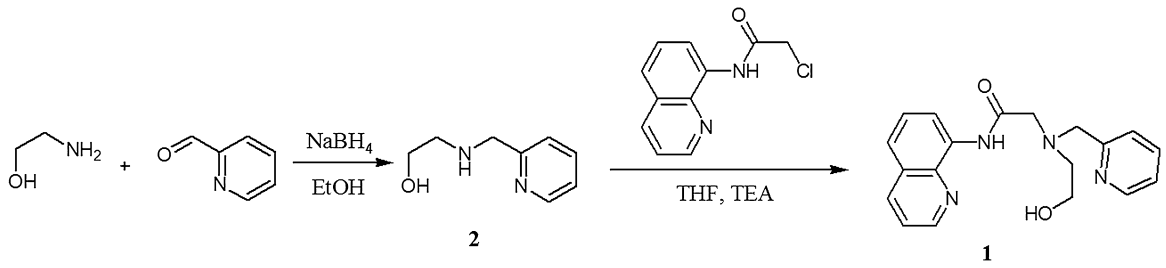

Scheme 1. Synthesis of sensor **1**.

solution, and sensed quantitatively Zn^{2+} in the water samples and living cells for practical application.

2. Experimental

2.1. Materials and instrumentation

All the solvents and reagents (analytical grade and spectroscopic grade) were obtained commercially and used as received. NMR spectra were recorded on a Varian 400 spectrometer. Chemical shifts (δ) are reported in ppm, relative to tetramethylsilane $Si(CH_3)_4$. Absorption spectra were recorded at 25 °C using a Perkin Elmer model Lambda 25 UV/vis spectrometer. The emission spectra were recorded on a Perkin-Elmer LS45 fluorescence spectrometer. Electrospray ionization mass spectra (ESI–MS) were collected on a Thermo Finnigan (San Jose, CA, USA) LCQTM Advantage MAX quadrupole ion trap instrument. Elemental analysis for carbon, nitrogen, and hydrogen was carried out by using a Flash EA 1112 elemental analyzer (thermo) in Organic Chemistry Research Center of Sogang University, Korea.

2.2. Synthesis of sensor *1*

2-Aminoethanol (10 mmol, 0.97 mL) and picolinaldehyde (10 mmol, 0.61 mL) were dissolved in ethanol (15 mL) and stirred for 3 h. Then, $NaBH_4$ (10.2 mmol, 0.38 g) was added, and the reaction solution was cooled in an ice bath. It was stirred for 2 h and the solvent was removed under reduced pressure to obtain colorless oil (**2**) (Scheme 1). The colorless oily residue (**2**) was dissolved in methylene chloride and then the solution was washed twice with water. Organic layer was dried over anhydrous Na_2SO_4 and the solvent was evaporated under vacuo. The resultant product **2** (2 mmol, 0.3 g), 2-chloro-*N*-(quinolin-8-yl)acetamide (2.2 mmol, 0.49 g) and triethylamine (TEA, 2 mmol, 0.28 mL) were dissolved in tetrahydrofuran (THF, 30 mL), stirred and refluxed for 1 d. The mixture was cooled down to room temperature and the solvent was removed under reduced pressure to obtain brown oil, which was purified by silica gel column chromatography (9: 1 v/v $CHCl_3$—CH_3OH). Yield: 0.49 g (73%). ^{1}H NMR (400 MHz, DMSO-d_6, 25 °C): δ = 11.45 (s, 1*H*), 9.01 (d, *J* = 4 Hz, 1*H*), 8.68 (d, *J* = 4 Hz, 1*H*), 8.49 (d, *J* = 4 Hz, 1*H*), 8.43 (d, *J* = 8 Hz, 1*H*), 8.01(d, *J* = 8 Hz, 1*H*), 7.85 (t, *J* = 6 Hz, 1*H*), 7.67 (m, 2*H*), 7.59 (t, *J* = 8 Hz, 1*H*), 7.23 (t, *J* = 10 Hz, 1*H*), 4.60 (t, *J* = 5 Hz, 1*H*), 3.98 (s, 2*H*), 3.63 (m, 2*H*), 3.53 (s, 2*H*), 2.71 (t, *J* = 6 Hz, 2*H*) ppm. ^{13}C NMR (100 MHz, DMSO-d_6, 25 °C): δ = 169.66, 158.58, 149.02, 148.70, 137.93, 136.63, 136.56, 134.02, 127.83, 127.02, 122.95, 122.30, 122.21, 121.70, 115.40, 61.49, 60.16, 59.32, 56.77 ppm. LRMS (ESI): *m*/*z* calcd for $C_{19}H_{20}N_4O_2 + H^+$: 337.17; found 337.10. Elemental analysis calcd (%) for $C_{19}H_{20}N_4O_2$: C, 67.84; H, 5.99; N, 16.66; found: C, 67.65; H, 5.95; N, 16.75.

2.3. UV–vis titration of *1* with Zn^{2+}

Sensor **1** (0.50 mg, 0.0015 mmol) was dissolved in MeOH (0.5 mL) and 10 μL of the sensor **1** (3 mM) were diluted to 2.990 mL bis–tris buffer solution (10 mM, pH 7.0) to make the final concentration of 10 μM. $Zn(NO_3)_2$ (0.01 mmol) was also dissolved in bis–tris buffer solution (1 mL) and 0.6–12 μL of the Zn^{2+} solution (5 mM) were transferred to separate sensor solutions (10 μM, 3 mL). After mixing them for a few seconds, UV–vis spectra were taken at room temperature.

2.4. Fluorescence titration of *1* with Zn^{2+}

Sensor **1** (0.50 mg, 0.0015 mmol) was dissolved in MeOH (0.5 mL) and 10 μL of the sensor **1** (3 mM) were diluted to 2.990 mL bis–tris buffer solution (10 mM, pH 7.0) to make the final concentration of 10 μM. $Zn(NO_3)_2$ (0.01 mmol) was also dissolved in bis–tris buffer solution (1 mL) and 0.6–6 μL of the Zn^{2+} solution (5 mM) were added to the sensor **1** solution (10 μM, 3 mL) prepared above. After mixing them for a few seconds, fluorescence spectra were obtained at room temperature.

2.5. NMR titration of *1* with Zn^{2+}

Three NMR tubes of **1** (0.67 mg, 0.002 mmol) dissolved in CD_3OD (0.5 mL) were prepared, and three different equivalents (0, 0.5, and 1 equiv) of zinc nitrate dissolved in CD_3OD (0.5 mL) were added separately to the solutions of **1**. After shaking them for a few seconds, the ^{1}H NMR spectra were taken.

2.6. Determination of Zn^{2+} in water samples

Fluorescence spectra measurement of water samples containing Zn^{2+} were carried by adding 20 μL of 3 mmol/L stock solution of **1** and 0.60 mL of 50 mmol/L bis–tris buffer stock solution to 2.38 mL sample solutions. After well mixed, the solutions were allowed to stand at 25 °C for 2 min before test.

2.7. Methods of cell test of *1* with Zn^{2+}

Human dermal fibroblast cells in low passage were cultured in FGM-2 medium (Lonza, Switzerland) supplemented with 10% fetal bovine serum, 1% penicillin/streptomycin in the in vitro incubator with 5% CO_2 at 37 °C. Cells were seeded onto a 8 well plate (SPL Lifesciences, Korea) at a density of 2×10^5 cells per well and then incubated at 37 °C for 4 h after addition of various concentrations (0–200 μM) of $Zn(NO_3)_2$ dissolved in MeOH. After washing with phosphate buffered saline (PBS) two times to remove the remaining $Zn(NO_3)_2$, the cells were incubated with **1** (30 μM) dissolved in MeOH at room temperature for 30 min. The cells were observed using a microscope (Olympus, Japan). The fluorescent images of the cells were obtained using a fluorescence microscope (Leica DMLB, Germany) at the excitation wavelength of 425 nm. The mean fluorescence intensity of the microscopy images in Fig. 6 was evaluated by Icy software [10].

2.8. Live/dead assay of fibroblast with **1**

To observe cell viability, live & dead assays were performed for **1** and **1**-Zn^{2+}, respectively. Fibroblasts ($P = 5$) were in vitro cultured to reach 70% confluent. For **1**, the cells were incubated with **1** (30 μM) dissolved in MeOH for 1, 12, and 24 h. Reagent (400 μL) of the live & dead assay was added into each cell culture plate. For **1**-Zn^{2+}, the cells were incubated for 4 h after addition of $Zn(NO_3)_2$ (100 μM) dissolved in MeOH. After washing with phosphate buffered saline (PBS) two times to remove the remaining $Zn(NO_3)_2$, the cells were incubated with **1** (30 μM) dissolved in MeOH for 1, 12, and 24 h at room temperature. Both viability and morphological changes of the cells were observed by a fluorescence microscope (Leica DMLB, Leica; Wetzlar, Germany).

2.9. Methods of theoretical calculations

All Theoretical calculations were performed by using Gaussian 03 suite [11]. The singlet ground states (S_0) of **1** and **1**$^{-}$-Zn^{2+} complex were optimized by DFT methods with Becke's three parameterized Lee-Yang-Parr (B3LYP) exchange functional with 6 – 31 + G** basis set [12]. In vibrational frequency calculations, there is no imaginary frequency for **1** and **1**$^{-}$-Zn^{2+} complex, suggesting that the optimized **1** and **1**$^{-}$-Zn^{2+} complex represent local minima.

3. Results and discussion

3.1. Synthesis of 1

The compound **2** (2-((pyridin-2-yl)methylamino)ethanol) was synthesized by condensing 2-aminoethanol and picolinaldehyde in ethanol (Scheme 1). Subsequently, the substitution reaction of **2** to 2-chloro-*N*-(quinolin-8-yl)acetamide afforded the sensor **1**, which was characterized by ^{1}H NMR, ^{13}C NMR, ESI-mass spectrometry (Figs. S1–3) and elemental analysis.

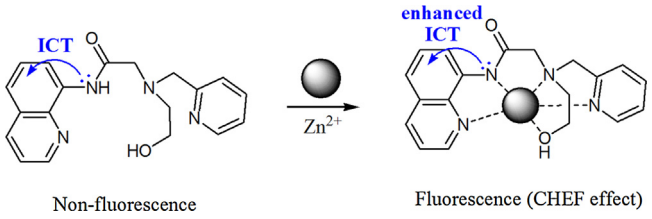

Scheme 2. Fluorescence enhancement mechanism and proposed structure of **1** in the presence of Zn^{2+}.

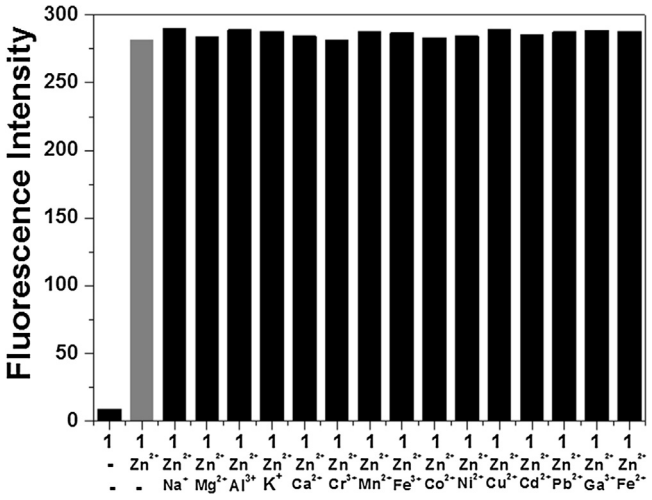

Fig. 2. Competitive selectivity of **1** (10 μM) toward Zn^{2+} (1 equiv) in the presence of other metal ions (1 equiv) with an excitation of 356 nm in buffer solution (10 mM bis–tris, pH 7.0).

3.2. Fluorescence and absorption spectroscopic studies of **1** toward Zn^{2+}

The fluorometric behavior of sensor **1** toward various metal ions was studied in bis–tris buffer solution (10 mM, pH 7.0).

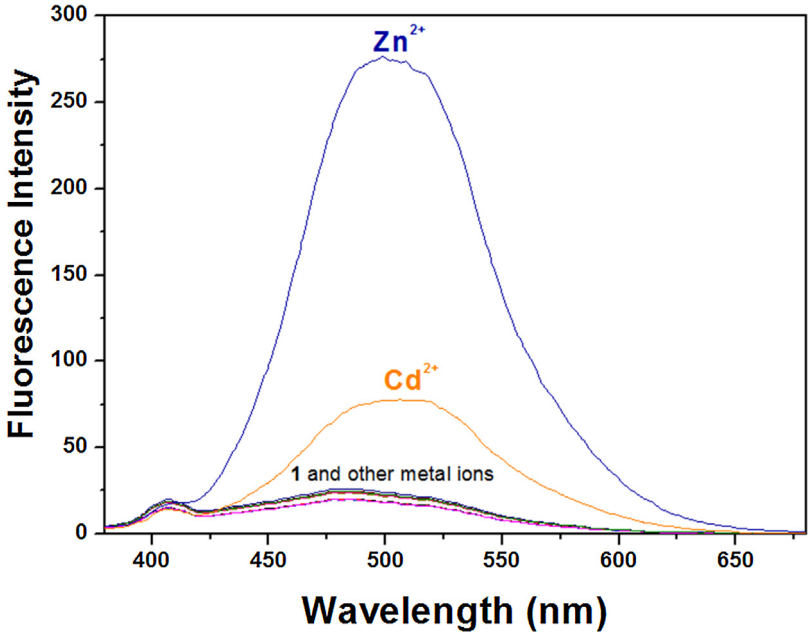

Fig. 1. Fluorescence spectra changes of **1** (10 μM) in the presence of different metal ions (1 equiv) such as Na^{+}, K^{+}, Mg^{2+}, Ca^{2+}, Al^{3+}, Ga^{3+}, Cr^{3+}, Mn^{2+}, Fe^{2+}, Fe^{3+}, Co^{2+}, Ni^{2+}, Cu^{2+}, Zn^{2+}, Cd^{2+} and Pb^{2+} with an excitation of 356 nm in buffer solution (10 mM bis–tris, pH 7.0).

When excited at 356 nm, **1** exhibited a weak fluorescence emission (λ_{max} = 500 nm) with a low quantum yield (Φ = 0.00672), which was much lower than that (Φ = 0.0682) in the presence of Zn^{2+} (Fig. 1). By contrast, upon addition of other metal ions such as Na^{+}, K^{+}, Mg^{2+}, Ca^{2+}, Al^{3+},Ga^{3+}, Cr^{3+}, Mn^{2+}, Fe^{2+}, Fe^{3+}, Co^{2+}, Ni^{2+}, Cu^{2+}, Zn^{2+}, Cd^{2+} and Pb^{2+}, either no or slight increase in intensity were observed. Meanwhile, the addition of Cd^{2+} into **1** also showed the increase in the fluorescence intensity at 510 nm. However, the intensity was small compared to the high fluorescence enhancement of the receptor in the presence of Zn^{2+}. These results indicate that sensor **1** could be used as a fluorescence chemosensor for Zn^{2+}.

To further investigate the chemosensing properties of **1**, fluorescence titration of the sensor **1** with Zn^{2+} ion was performed. As shown in Fig. S4, the emission intensity of **1** at 500 nm steadily increased with a slight red shift from 490 to 500 nm until the amount of Zn^{2+} reached 1 equiv. The photophysical properties of **1** were also examined using UV–vis spectrometry. UV–vis absorption spectrum of **1** showed two absorption bands at 245 and 312 nm (Fig. S5). Upon the addition of Zn^{2+} ions to a solution of **1**, the two bands have red-shifted to 259 and 353 nm, respectively. Meanwhile, three clear isosbestic points were observed at 251, 286 and 332 nm, implying the undoubted conversion of free **1** to a zinc complex.

Fluorescence and UV–vis spectroscopic studies led us to propose that the red shift of **1**-Zn^{2+} complex was induced by the enhancement of ICT (intramolecular charge transfer) band [2b,13]. Moreover, the complexation of **1** with Zn^{2+} would make **1** more rigid, thus resulting in a chelation-enhanced fluorescence (CHEF) effect as depicted in Scheme 2.

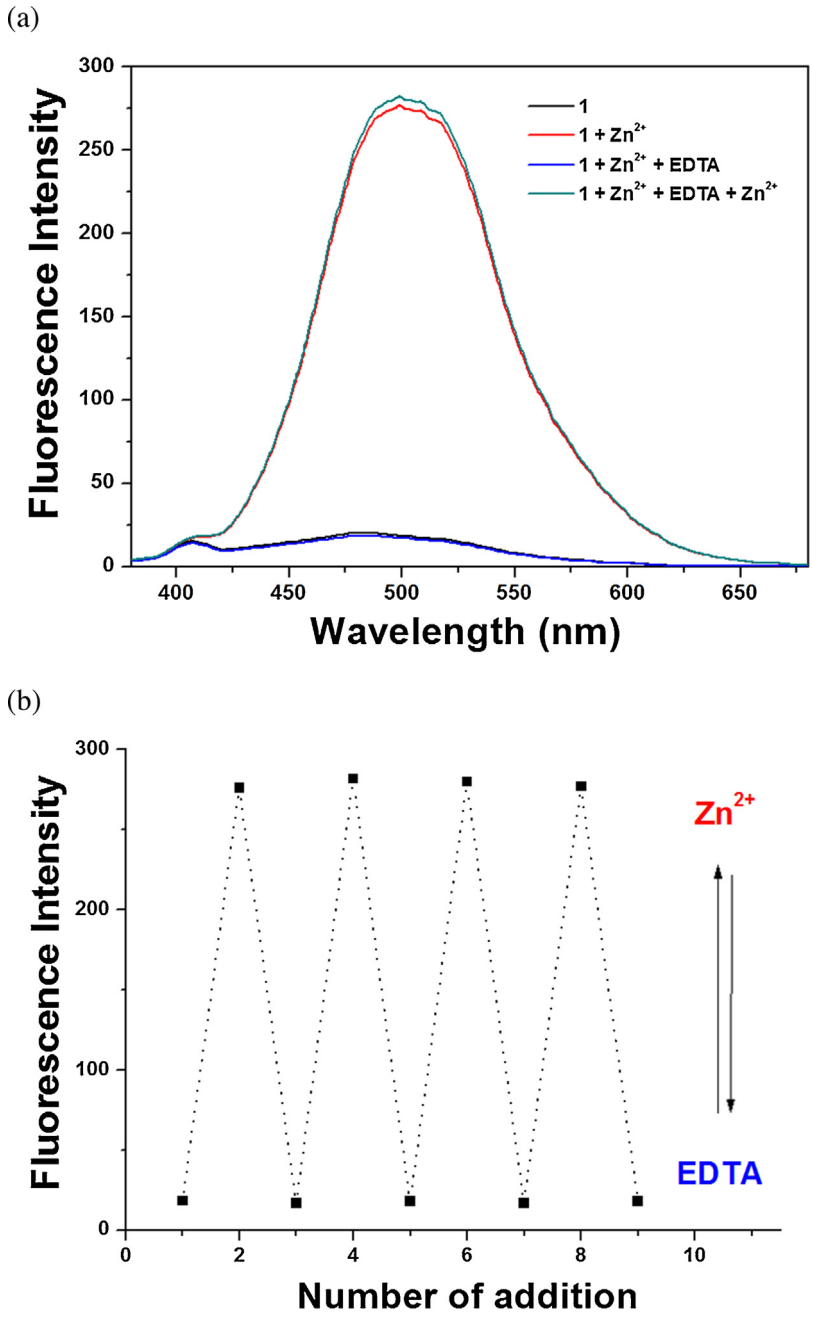

Fig. 3. (a) Fluorescence spectral changes of **1** (10 μM) after the sequential addition of Zn^{2+} and EDTA in buffer solution (10 mM bis–tris, pH 7.0). (b) Reversible changes in fluorescence intensity of **1** (10 μM) at 500 nm after the sequential addition of Zn^{2+} and EDTA.

The Job plot showed a 1:1 complexation stoichiometry between **1** and Zn^{2+} (Fig. S6) [14], which was further confirmed by ESI–mass spectrometry analysis (Fig. S7). The positive-ion mass spectrum of **1** upon addition of 1 equiv of Zn^{2+} showed the formation of the **1**-H^+ + Zn^{2+} [*m*/*z*: 399.06; calcd, 399.08]. Based on pK_a values (11.9 vs 15.8) of the acetamide and ethanol moieties reported in the literatures [15], we proposed that the proton of the amide moiety might be deprotonated when **1** coordinated to Zn^{2+} as shown in Scheme 2. From the UV–vis titration data, the association constant for **1** with Zn^{2+} was determined as 5.0 ($\pm$0.1) $\times$ 10^7 M^{-1} using Benesi–Hildebrand equation (Fig. S8) [16]. This value is within the range of those (1.0–1.0 $\times$ 10^{12}) reported for Zn^{2+} sensing chemosensors [17]. To check the possible interference of other metal ions on zinc complexation with sensor **1**, competition experiments were performed in the presence of Zn^{2+} mixed with various metal ions. When **1** was treated with 1 equiv of Zn^{2+} in the presence of other metal ions of the same concentration (Fig. 2), other background metal ions had no obvious interference with the detection of Zn^{2+} ion. In particular, Cd^{2+} ion hardly inhibited the emission intensity of **1**-Zn^{2+}. These results indicate that **1** could be a good Zn^{2+} sensor which could distinguish Zn^{2+} from Cd^{2+} commonly having similar properties.

3.3. ^{1}H NMR spectroscopic studies of **1** toward Zn^{2+}

The ^{1}H NMR titration experiments were studied to further examine the binding mode between **1** and Zn^{2+} ion (Fig. S9). Upon addition of Zn^{2+} to sensor **1**, the protons H_2, H_9, H_{10}, H_{11}, H_{12}, and H_{16} showed downfield shift, while a slight up-field shift was observed for H_7. These chemical shifts suggest that the oxygen atom of the ethanol moiety and the four nitrogen atoms might coordinate to Zn ion (Scheme 2). This coordinative behavior of potentially

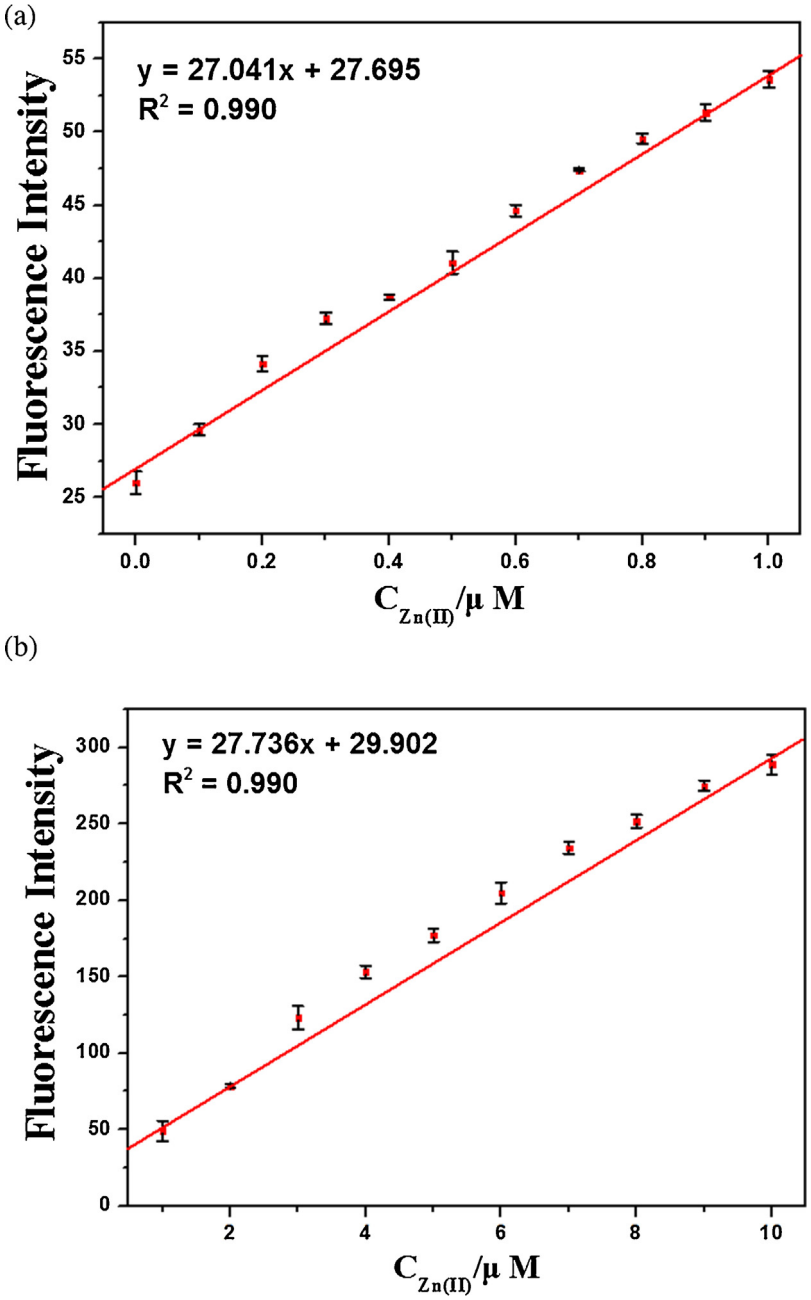

Fig. 4. Fluorescence intensity (at 500 nm) of **1** as a function of Zn(II) concentration. (a) [**1**] = 10 μmol/L, [Zn(II)] = 0–1.00 μmol/L; (b) [**1**] = 20 μmol/L, [Zn(II)] = 1.00–10.00 μmol/L. Conditions: all samples were conducted in buffer–MeOH solution (999:1, 10 mM bis–tris, pH 7.0). λ_{ex} and λ_{em} were 356 and 500 nm, respectively.

Table 1
Determination of Zn(II) in water samples.

Sample	Zn(II) added (μmol/L)	Zn(II) found (μmol/L)	Recovery (%)	R.S.D. (n = 3) (%)
Tap water	0.00	0.00		
	8.00	7.57	94.6	2.6
Water sample[a]	0.00	6.62	110.3	1.5
	2.00	8.43	105.4	2.4

[a] Synthesized by deionized water, 6.00 μmol/L Zn(II), 10 μmol/L Cd(II), Pb(II), Na(I), K(I), Ca(II), Mg(II). Conditions: [**1**] = 20 μmol/L in 10 mM bis–tris buffer–MeOH solution (999:1, pH 7.0).

penta-dentate ligand **1** with a zinc ion was previously observed in the similar type of zinc complexes [18]. There was no shift in the position of proton signals on further addition of Zn^{2+} (>1.0 equiv), which indicated the 1:1 ratio of **1**-Zn^{2+} complex. Based on Job plot, ESI–mass spectrometry analysis, ^{1}H NMR titration, and the crystal structures of similar types of zinc complexes, we propose the structure of **1**-Zn^{2+} complex as shown in Scheme 2.

3.4. pH effect of *1* toward Zn^{2+}

To study the practical applicability of this chemosensor, the effects of pH on the fluorescence response of Zn^{2+} were investigated (Fig. S10). The fluorescence spectra of sensor **1** in the absence and presence of 1 equiv of Zn^{2+} were examined at pH ranging from 2 to 12. The fluorescence intensity of **1** in the presence of Zn^{2+} showed a response between pH 3 and 12. In particular, the sharp absorbance increase between pH 4 and 5 indicated that the proton of the acetamide group in **1**-Zn^{2+} complex began to deprotonate (pK_a = 4.54) [19]. These results indicate that Zn^{2+} could be clearly detected by the fluorescence spectra measurement using **1** over the environmentally and physiologically relevant pH range (pH 6.0–8.4) [20], especially for monitoring Zn^{2+} in water samples and living cells.

3.5. Reversible test of *1* toward Zn^{2+} by using EDTA

To examine the reversibility of sensor **1** toward Zn^{2+} in buffer solution, ethylenediaminetetraacetic acid (EDTA, 1 equiv) was added to the complexed solution of sensor **1** and Zn^{2+}. As shown in Fig. 3, a fluorescence signal at 500 nm was immediately quenched. Upon addition of Zn^{2+} again, the fluorescence was recovered. The fluorescence emission changes were almost reversible even after several cycles with the sequentially alternative addition of Zn^{2+} and EDTA. These results indicate that sensor **1** could be recyclable simply through treatment with a proper reagent such as EDTA. Such reversibility and regeneration could be important for the fabrication of chemosensors to sense Zn^{2+}.

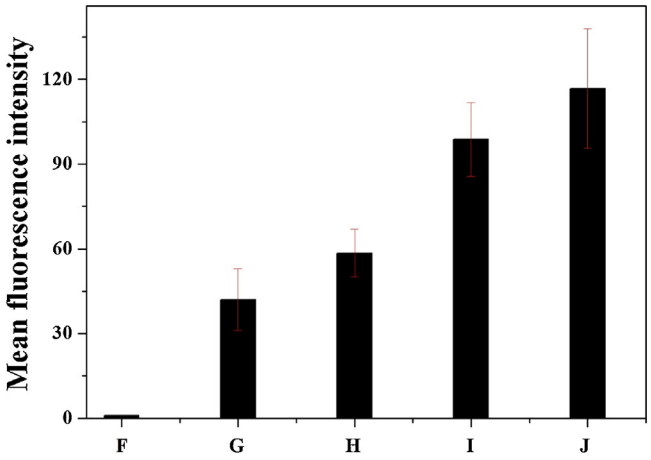

Fig. 6. Quantification of mean fluorescence intensity in Fig. 5 (F, G, H, I and J) correspondingly.

3.6. Analytical figures of merit

We constructed the calibration curves for the determination of Zn^{2+} by **1** (Fig. 4). Sensor **1** exhibited good linear relationships between the fluorescence intensity of **1** and Zn^{2+} concentration (0.10–10.00 μM) with correlation coefficients of R^2 = 0.990 (n = 3), which mean that **1** is suitable for quantitative detection of Zn^{2+}. The relative standard deviation (n = 3) is 5.72% at 0.6 μM Zn(II). The detection limit has also been calculated as 0.02 μM based on the definition by IUPAC ($C_{DL} = 3S_b/m$) (Table S1), which is thousand fold lower than the WHO guideline (76 μM) for Zn^{2+} ions in drinking water [21]. Importantly, this is the second lowest one for sensing of Zn^{2+} by fluorescence enhancement in a fully aqueous solution, to the best of our knowledge (Table S2).

3.7. Determination of zinc ion in water samples

In order to examine the applicability of the chemosensor **1** in environmental samples, the chemosensor was applied to the determination of Zn^{2+} in water samples. First, tap water samples were chosen. As shown in Table 1, one can see that the satisfactory recovery and R.S.D. values of water samples were exhibited. Also, we prepared artificial polluted water samples by adding various metal ions known as being involved in industrial processes into deionized

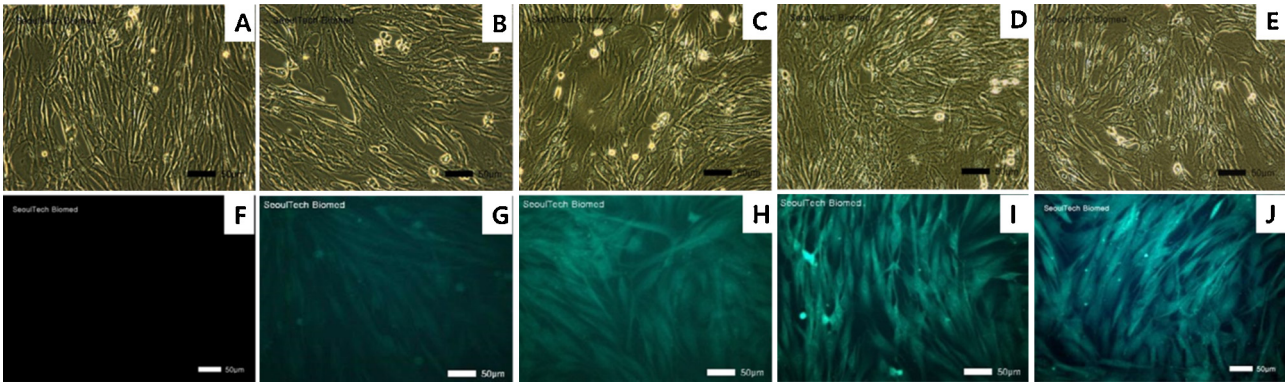

Fig. 5. Fluorescence images of fibroblasts cultured with Zn^{2+} and **1**. Cells were exposed to 0 (A and F), 10 (B and G), 40 (C and H), 100 μM (D and I) and 200 μM (E and J) $Zn(NO_3)_2$ for 4 h and then later with **1** (30 μM) for 30 m. The top images (A–E) were observed with the light microscope and the bottom images (F–J) were taken with a fluorescence microscope. The scale bar is 50 μm.

water. The results were also summarized in Table 1, which exhibited the satisfactory recovery and R.S.D. values for all the water samples.

3.8. Biological application for Zn^{2+}

To further demonstrate the potential of **1** to monitor Zn^{2+} in living matrices, fluorescence imaging experiments were carried out in living cells (Fig. 5). Adult human dermal fibroblasts were first incubated with various concentrations of aqueous Zn^{2+} solutions (0, 10, 40, 100 and 200 μM) for 4 h and then exposed to **1** for 30 min before imaging. The experimental results showed that the fibroblast cells without either Zn^{2+} or **1** showed negligible intracellular fluorescence, while those cultured with both Zn^{2+} and **1** exhibited fluorescence. With an increase in Zn^{2+} concentration from 10 to 200 μM, the fluorescence intensity of the cells with **1** increased. The mean fluorescence intensity of the microscopy image in Fig. 5 was evaluated by Icy software (Fig. 6). Moreover, the biocompatibilities of **1** and **1**-Zn^{2+} complex were examined with the living cells (Fig. 7). All the fibroblasts were still alive until 12 h for both **1** and **1**-Zn^{2+} complex, while a few cells were dead after 24 h. These observations confirm that **1** and **1**-Zn^{2+} complex could be suitable and biocompatible to detect and quantify Zn^{2+} in living cells.

3.9. Theoretical calculations

To obtain a deeper insight into the interaction of **1** with Zn^{2+}, theoretical calculations were carried out in parallel to the experimental studies. We performed all theoretical calculations by 1:1 stoichiometry, based on Job plot, ESI–mass spectrometry analysis, and ^{1}H NMR titrations. As the proton of amide group in **1** was deprotonated by Zn^{2+}, we calculated the deprotonated product for **1**-Zn^{2+} complex. Energy-minimized structures (S_0) for **1** and $\mathbf{1}^-$-Zn^{2+} were optimized by applying density functional

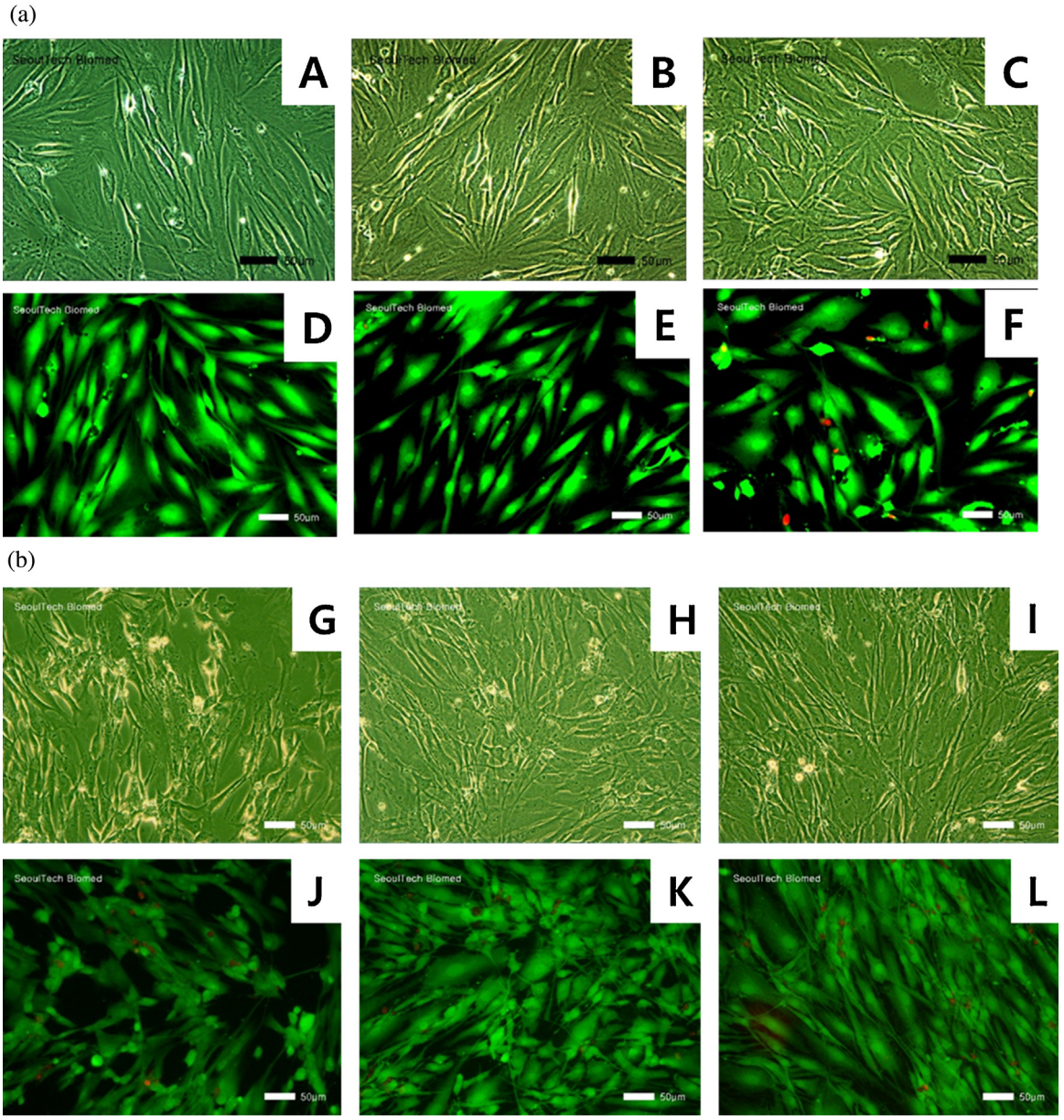

Fig. 7. Images of Live/Dead assays using fibroblasts with (a) **1** and (b) **1**-Zn^{2+}. The cells were incubated with (a) **1** and (b) **1**-Zn^{2+} dissolved in DMSO (**1**: 30 μM, Zn^{2+}: 100 μM) for 1 h (A, D, G and J), 12 h (B, E, H and K), and 24 h (C, F, I and L), respectively. Green color represents cells alive and red color for dead cells. The top images (A, B, C, G, H, and I) were observed using a light microscope, and the bottom images (D, E, F, J, K and L) were taken using a fluorescence microscope.

theory (DFT/B3LYP/6 – 31 + G**). The significant structural properties of the energy-minimized structures were indicated in Fig. S11. Based on the molecular orbitals (MOs) for the ground states of **1** and **1**$^{-}$-Zn^{2+} (Fig. S12), the chelation of Zn^{2+} with **1** rendered the HOMO to LUMO energy gap of **1** decrease, which is consistent with the red shift in the UV–vis spectrum and fluorescence emission of **1**$^{-}$-Zn^{2+}. Thus, these results demonstrate that ICT transition would contribute to the fluorescence enhancement of **1**-Zn^{2+}.

4. Conclusion

We synthesized a new ethyl alcohol-functionalized water-soluble based fluorescent chemosensor **1**, which displays high sensitivity and excellent selectivity toward zinc in aqueous solution. The binding of the sensor **1** and Zn^{2+} was chemically reversible with EDTA, and the detection limit (0.02 μM) is much lower than the WHO detection level (76 μM) for Zn^{2+} ions in drinking water. Most importantly, the recovery studies of the water samples added with Zn^{2+} and living cell experiments demonstrated its value in the practical application. Moreover, the theoretical calculations supported the sensing mechanism of Zn^{2+} by **1**, which was proposed with the combination of the increased ICT transitions and CHEF effects. Future study will focus on developing a chemosensor with the detection limit of picomolar level and its potential applications in biological chemistry.

Acknowledgements

Financial support from Basic Science Research Program through the National Research Foundation of Korea (NRF) funded by the Ministry of Education, Science and Technology (NRF-2014R1A2A1A11051794 and 2012008875) are gratefully acknowledged. We thank Nano-Inorganic Laboratory, Department of Nano & Bio Chemistry, Kookmin University to access the Gaussian 03 program packages.

Appendix A. Supplementary data

Supplementary data associated with this article can be found, in the online version, at http://dx.doi.org/10.1016/j.snb.2015.03.108

References

[1] (a) K.K. Upadhyay, A. Kumar, Pyrimidine based highly sensitive fluorescent receptor for Al^{3+} showing dual signalling mechanism, Org. Biomol. Chem. 8 (2010) 4892–4897;
(b) D. Karak, S. Lohar, A. Banerjee, A. Sahana, I. Hauli, S.K. Mukhopadhyay, J.S. Matalobos, D. Das, Interaction of soft donor sites with a hard metal ion: crystallographically characterized blue emitting fluorescent probe for Al(III) with cell staining studies, RSC Adv. 2 (2012) 12447–12454;
(c) Y.J. Lee, D. Seo, J.Y. Kwon, G. Son, M.S. Park, Y. Choi, J.H. Soh, H.N. Lee, K.D. Lee, J. Yoon, Anthracene derivatives bearing sulfur atoms or selenium atoms as fluorescent chemosensors for Cu^{2+} and Hg^{2+}: different selectivity induced from ligand immobilization onto anthracene, Tetrahedron 62 (2006) 12340–12344;
(d) M. Kumar, N. Kumar, V. Bhalla, Ratiometric nanomolar detection of Cu^{2+} ions in mixed aqueous media: a Cu^{2+}/Li^{+} ions switchable allosteric system based on thiacalix [4] crown, Dalton Trans. 41 (2012) 10189–10193;
(e) K.B. Kim, D.M. You, J.H. Jeon, Y.H. Yeon, J.H. Kim, C. Kim, A fluorescent and colorimetric chemosensor for selective detection of aluminum in aqueous solution, Tetrahedron Lett. 55 (2014) 1347–1352;
(f) K. Tayade, S.K. Sahoo, S. Chopra, N. Singh, B. Bondhopadhyay, A. Basu, N. Patil, S. Attarde, A. Kuwar, A fluorescent "turn-on" sensor for the biologically active Zn^{2+} ion, Inorg. Chim. Acta 421 (2014) 538–543;
(g) K. Tayade, S.K. Sahoo, R. Patil, N. Singh, S. Attarde, A. Kuwar, 2,2′-[Benzene-1,2-diylbis(iminomethanediyl)]diphenol derivative bearing two amine and hydroxyl groups as fluorescent receptor for Zinc(II) ion, Spectrochim. Acta, A 126 (2014) 312–316.

[2] (a) Z. Liu, C. Zhang, Y. Chen, W. He, Z. Guo, An excitation ratiometric Zn^{2+} sensor with mitochondria-targetability for monitoring of mitochondrial Zn^{2+} release upon different stimulations, Chem. Commun. 48 (2012) 8365–8657;
(b) Z. Xu, J. Yoon, D.R. Spring, Fluorescent chemosensors for Zn^{2+}, Chem. Soc. Rev. 39 (2010) 1996–2006;
(c) P. Jiang, Z. Guo, Fluorescent detection of zinc in biological systems: recent development on the design of chemosensors and biosensors, Coord. Chem. Rev. 248 (2004) 205–229;
(d) Y.W. Choi, G.J. Park, Y.J. Na, H.Y. Jo, S.A. Lee, G.R. You, C. Kim, A single schiff base molecule for recognizing multiple metal ions: a fluorescence sensor for Zn(II) and Al(III) and colorimetric sensor for Fe(II) and Fe(III), Sens. Actuators, B 194 (2014) 343–352;
(e) C. Zhang, Z. Liu, Y. Li, W. He, X. Gao, Z. Guo, In vitro and in vivo imaging application of a 1,8-naphthalimide-derived Zn^{2+} fluorescent sensor with nuclear envelope penetrability, Chem. Commun. 49 (2013) 11430–11432;
(f) Z. Guo, G. Kim, I. Shin, J. Yoon, A cyanine-based fluorescent sensor for detecting endogenous zinc ions in live cells and organisms, Biomaterials 33 (2012) 7818–7827.

[3] (a) T. Dudev, L. Carmay, Principles governing Mg, Ca, and Zn binding and selectivity in proteins, Chem. Rev. 103 (2003) 773–788;
(b) W.N. Lipscomb, N. Strater, Recent advances in zinc enzymology, Chem. Rev. 96 (1996) 2375–2433;
(c) R.K. Pathak, V.K. Hinge, D. Panda, C.P. Rao, Imino-phenolic-pyridyl conjugates of calix[4]arene (L_1 and L_2) as primary fluorescence switch-on sensors for Zn^{2+} in solution and in HeLa Cells and the recognition of pyrophosphate and ATP by [ZnL_2], Inorg. Chem. 51 (2012) 4994–5005;
(d) Y. Zhou, H.N. Kim, J. Yoon, A selective *'Off–On'* fluorescent sensor for Zn^{2+} based on hydrazine-pyrene derivative and its application for imaging of intracellular Zn^{2+}, Bioorg. Med. Chem. Lett. 20 (2010) 125–128;
(e) U. Fegade, H. Sharma, B. Bondhopadhyay, A. Basu, S. Attarde, N. Singh, A. Kuwar, Turn-on" fluorescent dipodal chemosensor for nano-molar detection of Zn^{2+}: application in living cells imaging, Talanta 125 (2014) 418–424;
(f) N. Khairnar, K. Tayade, S.K. Sahoo, B. Bondhopadhyay, A. Basu, J. Singh, N. Singh, V. Gite, A. Kuwar, A highly selective fluorescent 'turn-on' chemosensor for Zn^{2+} based on a benzothiazole conjugate: their applicability in live cell imaging and use of the resultant complex as a secondary sensor of CN^{-}, Dalton Trans. 44 (2015) 2097–2102.

[4] (a) H. He, D.K.P. Ng, Differential detection of Zn^{2+} and Cd^{2+} ions by BODIPY-based fluorescent sensors, Chem. Asian J. 8 (2013) 1441–1446;
(b) M. Hagimori, T. Uto, N. Mizuyama, T. Temma, Y. Yamaguchi, Y. Tominaga, H. Saji, Fluorescence ON/OFF switching Zn^{2+} sensor based on pyridine–pyridone scaffold, Sens. Actuators, B 181 (2013) 823–828;
(b) Z. Liu, C. Zhang, Y. Chen, F. Qian, Y. Bai, W. He, Z. Guo, In vivo ratiometric Zn^{2+} imaging in zebrafish larvae using a new visible light excitable fluorescent sensor, Chem. Commun. 50 (2014) 1253–1255;
(c) Z. Xu, G.H. Kim, S.J. Han, M.J. Jou, C. Lee, I. Shin, J. Yoon, An NBD-based colorimetric and fluorescent chemosensor for Zn^{2+} and its use for detection of intracellular zinc ions, Tetraderon 65 (2009) 2307–2312;
(e) K. Tayade, B. Bondhopadhyay, H. Sharma, A. Basu, V. Gite, S. Attarde, N. Singh, A. Kuwar, "Turn-on" fluorescent chemosensor for zinc(II) dipodal ratiometric receptor: application in live cell imaging, Photochem. Photobiol. Sci. 13 (2014) 1052–1057.

[5] (a) A.I. Bush, W.H. Pettingell, G. Multhaup, M. Paradis, J.P. Vonsattel, J.F. Gusella, K. Beyreuther, C.L. Masters, R.E. Tanzi, Rapid induction of Alzheimer a beta amyloid formation by zinc, Science 265 (1994) 1464–1467;
(b) V. Bhalla, M. Kumar, Pentaquinone based probe for nanomolar detection of zinc ions: chemosensing ensemble as an antioxidant, Dalton Trans. 42 (2013) 975–980.

[6] (a) K. Tayade, S.K. Sahoo, B. Bondhopadhyay, V.K. Bhardwaj, N. Singh, A. Basu, R. Bendre, A. Kuwar, Highly selective turn-on fluorescent sensor for nanomolar detection of biologically important Zn^{2+} based on isonicotinohydrazide derivative: application in cellular imaging, Biosens. Bioelectron. 61 (2014) 429–433;
(b) V.K. Gupta, N. Mergu, A.K. Singh, Fluorescent chemosensors for Zn^{2+} ions based on flavonol derivatives, Sens. Actuators, B 202 (2014) 674–682;
(c) M. Zhang, W. Lu, J. Zhou, G. Du, L. Jiang, J. Ling, Z. Shen, A simple and effective fluorescent chemosensor for the cascade recognition of Zn^{2+} and $H_2PO_4^{-}$ ions in protic media, Tetrahedron 70 (2014) 1011–1015;
(d) L. Qu, C. Yin, F. Huo, J. Chao, Y. Zhang, F. Cheng, A pyridoxal-based dual chemosensor for visual detection of copper ion and ratiometric fluorescent detection of zinc ion, Sens. Actuators, B 191 (2014) 158–164;
(e) W. Cao, X. Zheng, J. Sun, W. Wong, D. Fang, J. Zhang, L. Jin, A highly selective chemosensor for Al(III) and Zn(II) and its coordination with metal ions, Inorg. Chem. 53 (2014) 3012–3021.

[7] (a) R.E. Sturgeon, S.S. Berman, A. Desaulniers, D.S. Russell, Determination of iron, manganese, and zinc in seawater by graphite furnace atomic absorption spectrometry, Anal. Chem. 51 (1979) 2364–2369;
(b) R. Gulaboski, V. Mirčeski, F. Scholz, An electrochemical method for determination of the standard Gibbs energy of anion transfer between water and *n*-octanol, Electrochem. Commun. 4 (2002) 277–283;
(c) K.S. Rao, T. Balaji, T.P. Rao, Y. Babu, G.R.K. Naidu, Determination of iron, cobalt, nickel, manganese, zinc, copper, cadmium and lead in human hair by inductively coupled plasma-atomic emission spectrometry, Spectrochim. Acta, B 57 (2002) 1333–1338.

[8] (a) E.J. Song, J. Kang, G.R. You, G.J. Park, Y. Kim, S. Kim, C. Kim, R.G. Harrison, A single molecule that acts as a fluorescence sensor for zinc and cadmium and a colorimetric sensor for cobalt, Dalton Trans. 42 (2013) 15514–15520;
(b) K. Hanaoka, Y. Muramatsu, Y. Urano, T. Terai, T. Nagano, Design and synthesis of a highly sensitive off–on fluorescent chemosensor for zinc ions utilizing internal charge transfer, Chem. Eur. J. 16 (2010) 568–572;

(c) H.G. Lee, J.H. Lee, S.P. Jang, H.M. Park, S. Kim, Y. Kim, C. Kim, R.G. Harrison, Zinc selective chemosensor based on pyridyl-amide fluorescence, Tetrahedron 67 (2011) 8073–8078;
(d) S. Sinha, T. Mukherjee, J. Mathew, S.K. Mukhopadhyay, S. Ghosh, Triazole-based Zn^{2+}-specific molecular marker for fluorescence bioimaging, Anal. Chim. Acta 822 (2014) 60–68;
(e) D. Wang, X. Xiang, X. Yang, X. Wang, Y. Guo, W. Liu, W. Qin, Fluorescein-based chromo-fluorescent probe for zinc in aqueous solution: spirolactam ring opened or closed? Sens. Actuators, B 201 (2014) 246–254;
(f) Y. Ma, H. Chen, F. Wang, S. Kambam, Y. Wang, C. Mao, X. Chen, A highly sensitive and selective ratiometric fluorescent sensor for Zn^{2+} ion based on ICT and FRET, Dyes Pigm. 102 (2014) 301–307;
(g) N. Khairnar, K. Tayade, S. Bothra, S.K. Sahoo, J. Singh, N. Singh, R. Bendre, A. Kuwar, Novel fluorescent chemosensing of CN^- anions with nanomolar detection using the Zn^{2+}-isonicotinohydrazide metal complex, RSC Adv. 4 (2014) 41802–41806.

[9] (a) O. Akio, M. Yasuko, S. Kazuki, H. Itaru, Molecular recognition and fluorescence sensing of monophosphorylated peptides in aqueous solution by bis(zinc(II)-dipicolylamine)-based artificial receptors, J. Am. Chem. Soc. 126 (2004) 2454–2463;
(b) C. Lakshmi, R.G. Hanshaw, B.D. Smith, Fluorophore-linked zinc(II) dipicolylamine coordination complexes as sensors for phosphatidylserine-containing membranes, Tetrahedron 60 (2004) 11307–11315;
(c) B.A. Wong, S. Friedle, S.J. Lippard, Subtle modification of 2,2-dipicolylamine lowers the affinity and improves the turn-on of Zn(II)-selective fluorescent sensors, Inorg. Chem. 48 (2009) 7009–7011;
(d) A.J. Moro, P.J. Cywinski, S. Körsten, G.J. Mohr, An ATP fluorescent chemosensor based on a Zn(II)-complexed dipicolylamine receptor coupled with a naphthalimide chromophore, Chem. Commun. 46 (2010) 1085–1087;
(e) H. Kim, Y. Liu, D. Nam, Y. Li, S. Park, J. Yoon, M.H. Hyun, A new phosphorescent chemosensor bearing Zn-DPA sites for $H_2PO_4^-$, Dyes Pigm. 106 (2014) 20–24.

[10] F. de Chaumont, S. Dallongeville, N. Chenouard, N. Hervé, S. Pop, T. Provoost, V. Meas-Yedid, P. Pankajakshan, T. Lecomte, Y.L. Montagner, T. Lagache, A. Dufour, J. Olivia-Marin, Icy: an open bioimage informatics platform for extended reproducible research, Nat. Methods 9 (2012) 690–696.

[11] M.J. Frisch, G.W. Trucks, H.B. Schlegel, G.E. Scuseria, M.A. Robb, J.R. Cheeseman, J.A. Montgomery Jr., T. Vreven, K.N. Kudin, J.C. Burant, J.M. Millam, S.S. Iyengar, J. Tomasi, V. Barone, B. Mennucci, M. Cossi, G. Scalmani, N. Rega, G.A. Petersson, H. Nakatsuji, M. Hada, M. Ehara, K. Toyota, R. Fukuda, J. Hasegawa, M. Ishida, T. Nakajima, Y. Honda, O. Kitao, H. Nakai, M. Klene, X. Li, J.E. Knox, H.P. Hratchian, J.B. Cross, V. Bakken, C. Adamo, J. Jaramillo, R. Gomperts, R.E. Stratmann, O. Yazyev, A.J. Austin, R. Cammi, C. Pomelli, J.W. Ochterski, P.Y. Ayala, K. Morokuma, G.A. Voth, P. Salvador, J.J. Dannenberg, V.G. Zakrzewski, S. Dapprich, A.D. Daniels, M.C. Strain, O. Farkas, D.K. Malick, A.D. Rabuck, K. Raghavachari, J.B. Foresman, J.V. Ortiz, Q. Cui, A.G. Baboul, S. Clifford, J. Cioslowski, B.B. Stefanov, G. Liu, A. Liashenko, P. Piskorz, I. Komaromi, R.L. Martin, D.J. Fox, T. Keith, M.A. Al-Laham, C.Y. Peng, A. Nanayakkara, M. Challacombe, P.M.W. Gill, B. Johnson, W. Chen, M.W. Wong, C. Gonzalez, J.A. Pople, Gaussian 03, Revision D. 01, Gaussian, Inc., Wallingford, CT, 2004.

[12] (a) A.D. Becke, Density-functional thermochemistry. III. The role of exact exchange, J. Chem. Phys. 98 (1993) 5648–5652;
(b) J. Blaudeau, M.P. McGrath, L.A. Curtiss, L. Radom, Extension of Gaussian-2 (G2) theory to molecules containing third-row atoms K and Ca, J. Chem. Phys. 107 (1997) 5016–5021.

[13] (a) S. Aoki, K. Sakurama, N. Matsuo, Y. Yamada, R. Takasawa, S. Tanuma, M. Shiro, K. Takeda, E. Kimura, A new fluorescent probe for Zinc(II): an 8-hydroxy-5-*N*,*N*-dimethylaminosulfonylquinoline-pendant 1,4,7,10-tetraazacyclododecane, Chem. Eur. J. 12 (2006) 9066–9080;
(b) Z. Xu, K. Baek, H.N. Kim, J. Cui, X. Qian, D.R. Spring, I. Shin, J. Yoon, Zn^{2+}-triggered amide tautomerization produces a highly Zn^{2+}-selective, cell-permeable, and ratiometric fluorescent sensor, J. Am. Chem. Soc. 132 (2010) 601–610.

[14] P. Job, Formation and stability of inorganic complexes in solution, Ann. Chim. 9 (1928) 113–203.

[15] T. Heinze, T. Liebert, U. Heinze, K. Schwikal, Starch derivatives of high degree of functionalization 9: carboxymethyl starches, Cellulose 11 (2004) 239–245.

[16] H.A. Benesi, J.H. Hildebrand, A spectrometric investigation of the interaction of iodine with aromatic hydrocarbons, J. Am. Chem. Soc. 71 (1949) 2703–2707.

[17] (a) H.Y. Lin, P.Y. Cheng, C.F. Wan, A.T. Wu, A turn-on and reversible fluorescence sensor for zinc ion, Analyst 137 (2012) 4415–4417;
(b) J.H. Kim, I.H. Hwang, S.P. Jang, J. Kang, S. Kim, I. Noh, Y. Kim, C. Kim, R.G. Harrison, Zinc sensors with lower binding affinities for cellular imaging, Dalton Trans. 42 (2013) 5500–5507;
(c) W.H. Hsieh, C. Wan, D. Liao, A. Wu, A turn-on Schiff base fluorescence sensor for zinc ion, Tetrahedron Lett. 53 (2012) 5848–5851;
(d) Y. Zhou, Z. Li, S. Zang, Y. Zhu, H. Zhang, H. Hou, T.C.W. Mak, A novel sensitive turn-on fluorescent Zn^{2+} chemosensor based on an easy to prepare C3-symmetric Schiff-base derivative in 100% aqueous solution, Org. Lett. 14 (2012) 1214–1217.

[18] H.G. Lee, J.H. Lee, S.P. Jang, I.H. Hwang, S. Kim, Y. Kim, C. Kim, R.G. Harrison, Zinc selective chemosensors based on the flexible dipicolylamine and quinolone, Inorg. Chim. Acta 394 (2013) 542–551.

[19] (a) C.N. Baki, E.U. Akkaya, Boradiazaindacene-appended calix[4]arene: fluorescence sensing of pH near neutrality, J. Org. Chem. 66 (2001) 1512–1513;
(b) P. Mukerjee, K. Banerjee, A study of the surface pH of micelles using solubilized indicator dyes, J. Phys. Chem. 68 (1964) 3567–3574.

[20] R.M. Harrison, D.P.H. Laxen, S.J. Wilson, Chemical associations of lead, cadmium, copper, and zinc in street dusts and roadside soils, Environ. Sci. Technol. 15 (1981) 1378–1383.

[21] (a) Y.P. Kumar, P. King, V.S.K.R. Prasad, Zinc biosorption on Tectona grandis Lf leaves biomass: equilibrium and kinetic studies, Chem. Eng. J. 124 (2006) 63–70;
(b) K.B. Kim, H. Kim, E.J. Song, S. Kim, I. Noh, C. Kim, A cap-type Schiff base acting as a fluorescence sensor for zinc(II) and a colorimetric sensor for iron(II), copper(II), and zinc(II) in aqueous media, Dalton Trans. 42 (2013) 16569–16577;
(c) G.J. Park, Y.J. Na, H.Y. Jo, S.A. Lee, A.R. Kim, I. Noh, C. Kim, A single chemosensor for multiple analytes: fluorogenic detection of Zn^{2+} and OAc^- ions in aqueous solution, and an application to bioimaging, New J. Chem. 38 (2014) 2587–2594.

Biographies

Gyeong Jin Park earned the BS degree in 2013 at Seoul National University of Science and Technology. She is currently a Master Student at Seoul National University of Science and Technology. Her scientific interest includes chemical sensors, synthesis of catalyst and inorganic medicine.

Hyun Kim got her BS degree in 2012 at Seoul National University of Science and Technology. Then she is a MS candidate currently at Seoul National University of Science and Technology. Her major research interest includes chemical sensors and catalyst.

Jae Jun Lee earned the BS degree in 2014 at Seoul National University of Science and Technology. He is currently a Master Student at Seoul National University of Science and Technology. His scientific interest includes, molecular modeling, chemical sensors, and synthesis of catalyst.

Yong Sung Kim earned the BS degree in 2014 at Seoul National University of Science and Technology. He is currently a Master Student at Seoul National University of Science and Technology. His scientific interest includes chemical sensors, synthesis of catalyst and inorganic medicine.

Sun Young Lee earned the BS degree in 2014 at Seoul National University of Science and Technology. She is currently a Master Student at Seoul National University of Science and Technology. Her scientific interest includes reactivity study of the transition metal complexes and inorganic medicine.

Suyeon Lee received the BS degree in 2012 at Seoul National University of Science and Technology. She is currently a Master Student at Seoul National University of Science and Technology. Her research interests focus on tissue engineering.

Insup Noh is currently a Professor at Seoul National University of Science and Technology. He received the PhD degree in 1997 at University of Texas at Austin in USA. He is now interested in development of polymeric biomaterials for local delivery of bioactive agents and tissue engineering of bone, cartilage and nerve.

Cheal Kim is currently a professor at Seoul National University of Science and Technology. He received the PhD degree in 1993 at University of California, San Diego in USA. He is now interested in development of chemical sensors, reactivity study of the transition metal complexes, DNA cleavage by their metal complexes and MOF.